An ab Initio Study of the Interaction of SCN^- with a Silver Electrode: The Prediction of Vibrational Frequencies

F. Tielens, M. Saeys,[‡] E. Tourwé,[§] G. B. Marin,[‡] A. Hubin,[§] and P. Geerlings*[,†]

Eenheid Algemene Chemie (ALGC), Fakulteit Wetenschappen, Vrije Universiteit Brussel, Pleinlaan 2, B-1050 Brussels, Belgium, Laboratorium voor Petrochemische Techniek, Fakulteit Toegepaste Wetenschappen, Universiteit Gent, Krijgslaan 281 (S5), B-9000 Gent, Belgium, and Metallurgie, Elektrochemie en Materialenkennis (META), Fakulteit Toegepaste Wetenschappen, Vrije Universiteit Brussel, Pleinlaan 2, B-1050 Brussels, Belgium

Received: October 30, 2001

Experimental results for the adsorption frequencies of SCN^- on a silver electrode obtained with the surface-enhanced Raman spectrometry (SERS) method are presented and discussed. These results were confronted with a quantum chemical DFT-based study. Different clusters were used from the simple monoatomic case to a much more realistic representation of the silver electrode by means of a Ag_{23} cluster simulating the (100) surface. The calculations were performed at the B3PW91/LanL2DZ and the BP86/TZP level. The interaction energies indicate the importance of the cluster size and calculation level. The cluster size was increased until the results were converged. Calculated vibrational frequencies for the different possible adsorption geometries on a (100) surface are compared with experiment. Together with the interaction energy results, they indicate that the preferred interaction via the sulfur atom on a hollow site of the silver electrode is in agreement with the hard and soft acids and bases principle.

Introduction

The electroplating of silver plays a leading role in several branches of industry. Important applications are found in the formation of electronic contacts, the refining of metal household equipment and jewelry, and the production of lithographic plates for the offset printing on the base of the silver halide imaging technology.[1]

The formation of a silver image for imaging applications requires the electroreduction of complexed silver ions with SCN^- as a common complexing agent.[1−4] Adsorption of these anions at the growing silver deposit may influence the deposition process, which affects the final image quality[1,2,5−10]. The aim of the present study is to improve the insight into the silver electrodeposition process, because it is a fundamental part of the production of imaging systems and predominantly determines the image quality.

Even through the use of Raman and surface enhanced Raman (SER) spectroscopy,[10] there is still no certainty on the adsorption geometry of the adsorption complexes on a silver surface; quantum chemical calculations might help to cope with this problem. Besides elucidating the interaction of SCN^- with a silver-plated electrode (surface), the effect of the electrode potential on the adsorption behavior can also be investigated through quantum chemical calculations. The microscopic effect of the electrode potential is difficult to simulate and can have important consequences on the final adsorption geometry of SCN^-. Different methods have been proposed to study this extra charge effect such as the introduction of extra point charges, applying an electric field, or changing the charge of the cluster.[11−13] The major unknown in this problem is the absolute charge on each individual surface atom (or surface charge).

Quantum chemical investigations seem to give the most reliable evaluation of the interaction energies of the isolated ion−metal systems, because experimental techniques are often unable to provide the most important data such as the strength of the interaction of a single ion with the metal. Quantum chemically, one can treat the problem in two different ways:[14] the first approach being periodic calculation methods, such as periodic density functional theory (DFT) or crystal orbital Hartree−Fock (HF) and the second approach using a finite cluster model of the surface studied. It is the latter approach that will be used in this study, more precisely combined with DFT both computational and conceptual side.[15,16] Both approaches have their merits and limits.

Periodic calculations are more time-consuming, certainly if large unit cells are required. Large unit cells are necessary to avoid lateral interaction between adsorbed species.[17] Because in this study the adsorption of charged species is studied long range through space, lateral dipole interactions would necessitate the use of large unit cells.

On the other hand, cluster calculations are computationally less demanding (see, for example, the recent study by Seminario and co-workers on copper clusters),[18] although studies on larger clusters using large basis sets may still be prohibitive. For these computations, basis set convergence is important to obtain reliable adsorption energies. Another issue is the cluster size effect. The size and the way the clusters are constructed can have a large influence on the calculated absolute adsorption energies.[19] Therefore calculations on a series of clusters of different sizes are usually performed. Cluster calculations also allow the computation of analytical second derivatives of the energy for the computation of vibrational frequencies. This is

* To whom correspondence should be addressed. Tel: +32 2 629 33 14. Fax: +32 2 629 33 17. E-mail: pgeerlin@vub.ac.be.
† Eenheid Algemene Chemie (ALGC), Vrije Universiteit Brussel.
‡ Universiteit Gent.
§ Metallurgie, Elektrochemie en Materialenkennis (META), Vrije Universiteit Brussel.

10.1021/jp013992j CCC: $22.00
Published on Web 01/30/2002

not yet possible on a routine basis and certainly not commonly used[20] with periodic codes (for an overview of this matter, see refs 14 and 21).

The theoretical study of the interaction of ions on metal surfaces has been the subject of many theoretical papers, the most closely related studies being found in refs 11−13 and 22−26. However, only one theoretical study has treated the special case of the interaction of SCN^- with (a model of) a Ag electrode. This calculation was performed at the HF level on clusters of different size up to 10 Ag atoms.[27] In this particular study, only one interaction site was considered and no frequency analysis was performed. Because of computational limits, the authors could not predict which adsorption geometry was the most favorable because interaction energies were too close to each other. In contrast with former similar investigations on ions or molecules interacting with a metal surface, in the present study, a full quantum chemical (DFT level) calculation of the adsorbate is performed, as well as a full geometry optimization and frequency analysis for the adsorbate using different clusters to represent the different possible adsorption Ag-surface sites.

In the first part, the vibration frequencies and frequency shifts after interaction with Ag electrode were experimentally determined using SERS. In ref 10, a first step was already undertaken by some of the present authors to establish the nature of the silver complexes of SCN^- in the case of a single silver ion. Although the theoretical study was only done at the HF level with a 3-21G* basis set and using a single atom representation of the surface, the right trends for the frequency shifts were recovered and indications were found that the interaction of thiocyanate occurs via the sulfur atom.

In the second part, the latter trend will be explained and further investigated within the framework of conceptual DFT, in which our group has been active since the late eighties.[28−31] It will be seen that in this kind of interaction the hardness or softness of the interaction partner will play an important role.

Two properties of the adsorption complex were investigated using quantum chemical methods; the effect of the cluster size and adsorption site on the interaction energy of SCN^- was studied. Starting from a single atom representation, the cluster was enlarged to 23 silver atoms, passing an Ag_9 representation.

Experimental Details

Aqueous solutions of SCN^- were prepared by dissolving NaSCN (pro analyse (pa), UCB) in deionized water at pH 12 (NaOH, pa, Merck) and at 25 °C; 0.6 M $NaNO_3$ (pa, Merck) was added as an internal reference. Raman and SER spectra were recorded with a DILOR XY spectrograph with an energy resolution of about 2 cm^{-1}. The 514.5 nm line of an argon ion laser (American Laser, model LS1000) is used as the excitation line. The output power was 60 mW, giving about 15mW on the sample. The acquisition time was taken constant at 60 s for each spectrum. The SER substrate was a silver-plated polycrystalline silver disk electrode (radius 2 mm). The exact plating conditions were given earlier.[10] Potentials were applied with a high-resolution/stability potentiostat (Autolab PGSTAT10-Ecochemie) and referred to a calomel electrode with saturated KCl solution (SCE). A platinum rod served as the counter electrode.

Computational Details

To establish the nature of the silver-thiocyanate complex, full, and in some cases constrained, geometry optimizations of the SCN^- anion were performed using the UHF, UBP86,[32] and UB3PW91 method[33] in combination with different basis sets. Although the hybrid, nonlocal density functional B3PW91 was initially designed to reproduce thermodynamical properties of a series of mainly organic molecules, reasonable results can be found for transition metals as well.[34−38]

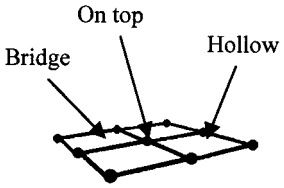

Figure 1. The different adsorption sites on a (100) surface.

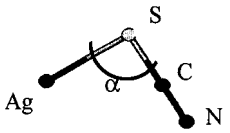

Figure 2. Adsorption geometry of SCN^- on the Ag_1 cluster.

Two types of DFT computations are considered. On the smaller clusters, hybrid DFT energy and frequency calculations have been done using the UB3PW91 functional and different basis sets. Because in some clusters opens shells are present, an unrestricted formalism is used. On both smaller and larger clusters, DFT computations using the unrestricted BP86 functional as implemented in the Amsterdam Density Functional (ADF2000) package[39] have been performed. In these calculations, molecular orbitals are represented by Slater-type functions. The innermost shells are kept frozen and replaced by an effective core potential. The extent of these frozen cores was up to and including the following shells: Ag 4p, S 2p, C 1s, and N 1s. The basis sets used, hereafter called TZP, were of triple-ζ quality augmented with two polarization functions. Relativistic effects were included with the zeroth order relativistic approximation (ZORA) Hamiltonian.[40] The completeness of this basis set was verified by basis set superposition error (BSSE) computations. On the Ag_5 cluster calculations, the BSSE was found to be less than 2 kJ/mol for the SCN basis set and less than 1 kJ/mol for the Ag basis. So, a counterpoise correction is not necessary for the ADF calculations, because the basis sets were large enough. All of these calculations have been done on a Linux Pentium PC.

On the smaller clusters, B3PW91 calculations with Pople basis sets[41] and the effective core potential LanL2DZ[42−44] are also used; the latter enabled us to obtain good quality geometries and interaction energies at lower calculation cost. The calculations, which have been carried out using the Gaussian 98[45] package, were done on a Compaq Digital DS20 workstation.

On the optimized geometries, frequency calculations are performed and interaction energies are calculated. Because the correction due to the inclusion of the counterpoise correction[46] significantly affects the results obtained with the Pople and LanL2DZ basis sets, the BSSE[47] was also calculated.

The adsorption on an ideal (100) surface can occur at three different sites, "on top" of a metal atom, between two metal atoms (bridge site), or in the middle of four metal atoms (hollow site), as shown in Figure 1. The Ag(100) surface has a surface atomic density intermediate between that of the compact (111) surface and that of the open (110) surface; because the reactivity of the surface depends on the surface atomic density,[48] the Ag(100) can be considered as possessing an average reactivity of different faces of the polycrystalline silver surface. The silver surface or silver electrode was modeled using different clusters (Figures 2−7). A single Ag atom to mimic an atop site, Ag_2 atoms to mimic the bridge site, a square of four Ag atoms to mimic the hollow site, a cross made of five Ag atoms to mimic

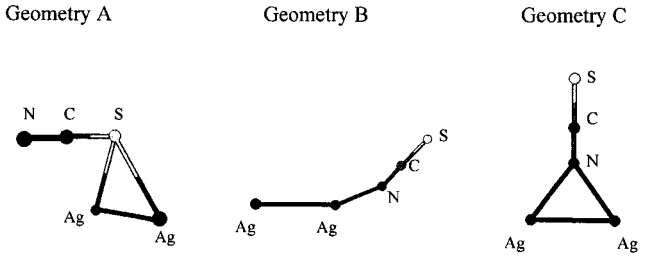

Figure 3. Adsorption geometries of SCN^- on the Ag_2 cluster.

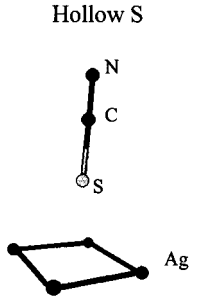

Figure 4. Adsorption of SCN^- on the Ag_4 cluster.

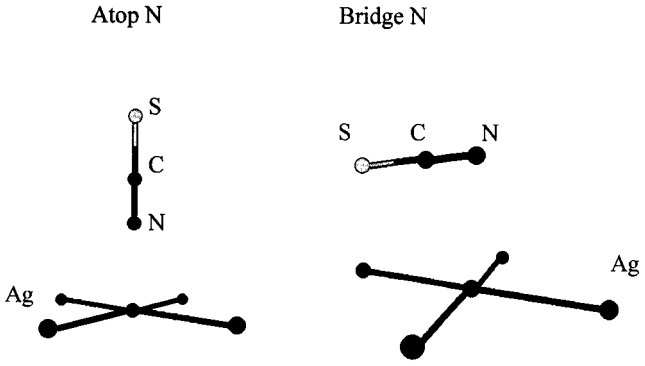

Figure 5. Adsorption of SCN^- on the Ag_5 cluster.

an atop site, and a double-layered cluster mimicking both hollow and atop sites formed by 9 Ag atoms were used. Finally, a Ag_{23} cluster was used to mimic the atop and hollow site on the (100) plane.

It should be noted that, although some structures are open-shell systems no problems of spin contamination will be encountered because DFT is a not a wave function based technique.[49] An important issue in cluster calculations are edge effects.[17] Edge atoms are coordinatively unsaturated and bind adsorbates much more strongly. Therefore, it is necessary to use large clusters for which the atoms building up the adsorption site are maximally coordinated. The largest cluster was constructed to satisfy this criterion. The Ag_{23} cluster has two layers. The top layer consists of 11 Ag atoms and has a maximum coordinated atop and bridge site to minimize the possible edge effects. The second layer consists of 12 Ag atoms to mimic a hollow site.

The geometries of all of the Ag clusters are kept rigid in the optimization to keep the geometry obtained by X-ray diffraction, which is a fcc structure with a cell constant of 408.53 pm,[50] (distance between Ag atoms on a (100) surface is 28.887 pm). The charge on the electrode is also varied because the net charge on the electrode is not known. The charge of the cluster was simulated by calculating the surface cluster with no extra charge and with one extra positive charge; in some cases, two extra charges were added. Because no fractional charges can be considered and knowing that the electrode is very low charged,

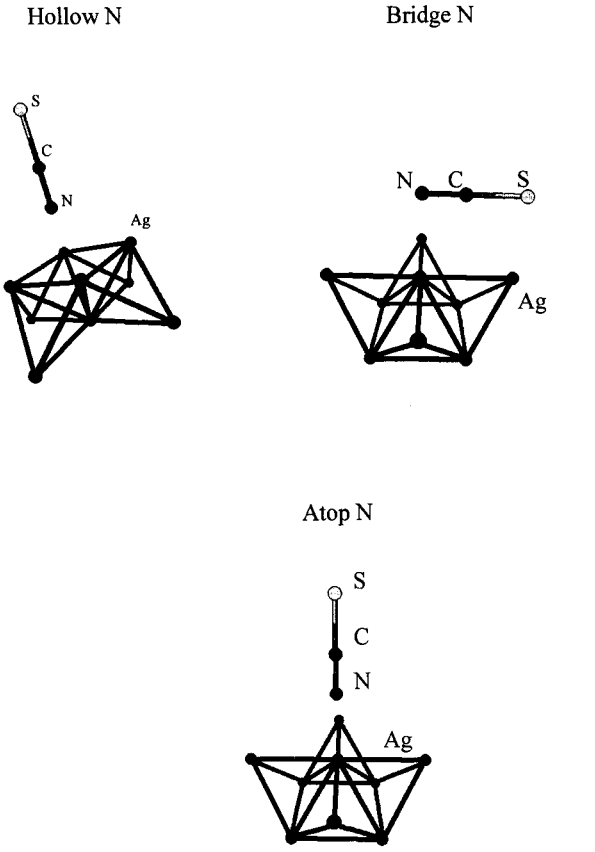

Figure 6. Adsorption of SCN^- on the Ag_9 cluster.

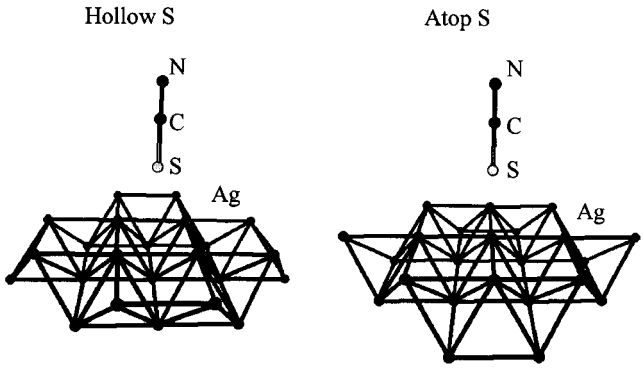

Figure 7. Adsorption of SCN^- on the Ag_{23} cluster.

the charge of the real electrode should be situated between the neutral and the +1 charged cluster. The real charge is presumed to be much closer to zero than to one. The validity of this assumption will be investigated in this study. The extra positive charge is spread out over the whole surface meaning that this charge converges to zero when a single atom is considered. On each cluster and adsorption site, the orientation of the adsorbate was varied, first considering the SCN^- interaction via the sulfur atom, second via its nitrogen atom, and in some cases via the carbon (i.e., parallel with the surface).

Results and Discussion

1. Experimental Results. The SER spectrum of a 10^{-3} M SCN^- solution is given in Figure 8. It shows three distinct peaks, which are attributed to the symmetric C−S stretching mode at 719 cm^{-1} (ν_2), the symmetric C≡N stretching mode at 2103 cm^{-1} (ν_3), and the S−C−N bending mode at 446 cm^{-1} (ν_1). It should be noted that the spectrum shows a sharp feature at 1045

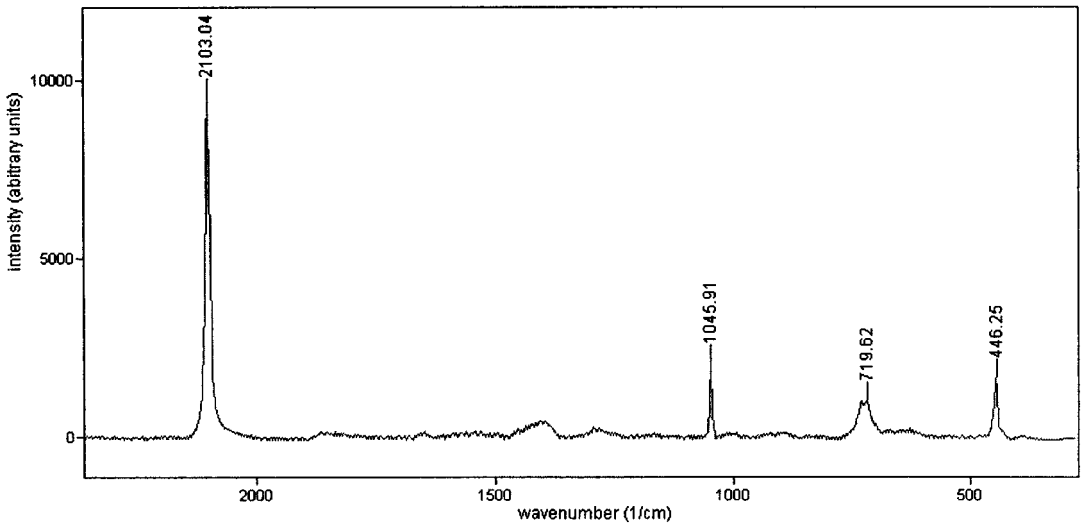

Figure 8. SER spectrum of SCN^- adsorbed on Ag at an applied potential of −0.2 V vs. SCE in an aqueous solution with a SCN^- concentration of 10^{-3} M.

TABLE 1: Wavenumbers, ν (in cm^{-1}), of the SER Peaks of a 10^{-3} M SCN^- Solution at Different Electrode Potentials (in mV vs SCE)

	−100	−200	−300	−400	−500
ν_1	446	446	447	443	447
ν_2	720	719	719	717	720
ν_3	2107	2103	2098	2093	2090

cm^{-1} due to the symmetric N−O stretch of the NO_3 internal reference molecule. This peak can be used to quantify the amount of SCN^- on the surface. Quantitative results will however not be discussed in this article.

In ref 10, the differences between the Raman and the SER spectrum of SCN^- are discussed. The most important ones are the shift in the SER spectrum of the ν_2 and ν_3 vibration modes compared to their counterparts in the Raman spectrum. The ν_2 mode shifts from 756 cm^{-1} (in the gas phase) to a lower wavenumber (719 cm^{-1} in Figure 8), and the ν_3 mode increases from 2059 cm^{-1} (in the gas phase) to a higher wavenumber (2103 cm^{-1} in Figure 8) after interaction with a silver surface. It is suggested that these differences are due to the interaction of SCN^- with the silver surface via the sulfur atom.[10] Peaks attributable to the formation of Ag−S bonding are however not observed in the SER spectrum, as the expected wavenumber is too low to be detected with the equipment used (cutoff of the used notch filter ca. 250 cm^{-1}). The adsorption of benzenethiol at silver, for instance, is accompanied by the appearance of a SER peak at 237 cm^{-1} due to the stretching of the Ag−S bond.[51]

To confirm the assumption that the interaction between SCN^- and silver occurs via the sulfur atom, the influence of the applied electrode potential on the SER spectrum of thiocyanate was studied. All spectra are similar to the one shown in Figure 8 but the peaks are slightly shifted. Table 1 lists the wavenumbers of these peaks for five different potentials. The ν_1 and ν_2 vibrations show a small shift of a few cm^{-1} as a function of potential. Because of limited resolution, it is not possible to conclude that these frequencies are influenced by the electrode potential value. The symmetric C≡N stretching vibration, on the other hand, shows a clear tendency as a function of the applied potential: when the potential becomes more negative, the frequency of this vibration decreases (see Figure 9).

The more negative the applied potential becomes, the more the ν_3 peak approaches its corresponding position in the Raman spectrum of the isolated molecule (i.e., before adsorption). This

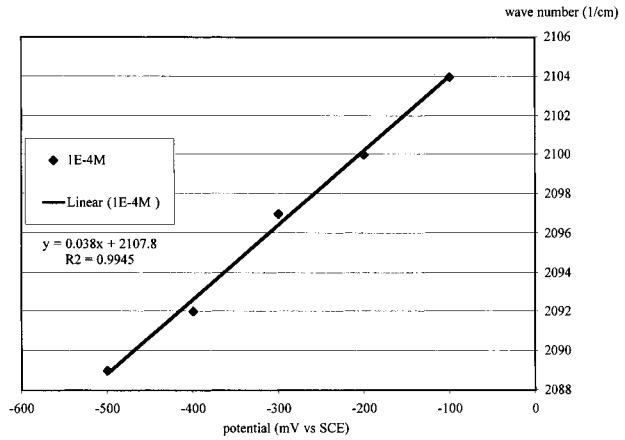

Figure 9. Evolution of the position of the ν(CN) mode as a function of the electrode potential (SCN^- concentration, 10^{-4} M).

should be due to a weakening of the C≡N bond, caused by a decline of the interaction strength between the adsorbed SCN^- molecules and the Ag surface as the potential becomes more negative. These experiments yield further indications on the interaction site of SCN^- with a silver electrode, which will now be completed with theoretical frequency shift studies.

2. Theoretical Results. *Building Up the Surface Cluster.* The simplest representation for a metal surface is only one surface atom. This procedure is known to neglect to many important effects, but nevertheless, for calculations of some special properties of the adsorbing molecule, such as vibration frequencies, this model can give already useful information, which was shown in ref 10. In this work, density functional theory is used in contrast with former studies in which HF was used. So, an assessment of the functional and basis set used is needed. The cluster was enlarged to 9 and 23 silver atoms. To study the influence of the calculation method as a function of the cluster size, the interacting systems were calculated with different basis sets and functionals.

The Simplest Representation. From the results in Table 2, one can conclude that the most favorable interaction on a Ag atom/ion occurs via the sulfur atom, shown by the most complete calculations (B3PW91/6-311+G*/3-21G, B3PW91/LanL2DZ, and BP86/TZP) (see Figure 2). Nevertheless, the B3PW91/6-311+G*/3-21G (−43.51 kJ/mol vs. −50.88 kJ/mol) result for the interaction with the neutral Ag shows an opposite trend with

TABLE 2: BSSE-Corrected Interaction Energies (ΔE in kJ/mol) and Geometry Parameters (angle in deg) of the $SCN^-\cdots Ag^q$ and $Ag^q\cdots SCN^-$ Complexes (with $q = 0$ or $+1$)

		basis set		S		N	
cluster	method	Ag	SCN^-	AgSC angle	ΔE	AgNC angle	ΔE
Ag	HF	3-21G	3-21G*	97.72	−53.60	164.72	−67.70
	B3PW91	3-21G	3-21G*	95.37	−52.55	164.73	−68.66
	B3PW91	3-21G	6-31G*	101.48	−49.54	164.14	−56.65
	B3PW91	3-21G	6-31+G*	104.88	−43.93	164.02	−50.46
	B3PW91	3-21G	6-311+G*	102.97	−43.51	164.17	−50.88
	B3PW91	LanL2DZ	LanL2DZ	105.65	−67.86	177.05	−65.14
	BP86	TZP	TZP	106.99	−69.66	163.83	−61.80
	HF[27]	ECP	ECP	107	−47.3	180	−61.7
Ag^+	HF	3-21G	3-21G*	86.09	−492.29	180.01	−497.23
	B3PW91	3-21G	3-21G*	86.72	−557.64	174.64	−558.56
	B3PW91	3-21G	6-31G*	85.38	−548.73	127.03	−543.96
	B3PW91	3-21G	6-31+G*	89.89	−534.92	158.26	−534.72
	B3PW91	3-21G	6-311+G*	88.14	−534.88	163.21	−534.51
	B3PW91	LanL2DZ	LanL2DZ	97.14	−598.56	145.65	−597.77
	BP86	TZP	TZP	98.52	−648.39	127.11	−636.30
	HF[27]	ECP	ECP	98	−498.8	180	−508.5

TABLE 3: BSSE-Corrected Interaction Energies (ΔE in kJ/mol) of SCN^- in Interaction with the Ag_4, Ag_5, Ag_9, and Ag_{23} Surface Clusters

		basis set					
cluster	method	Ag	SCN^-	interaction	hollow	atop	bridge
Ag_9	BP86	TZP	TZP	S		−34.12	−93.62
				N		−55.65	−96.25
				C		−52.81	
				S	−66.10		
				N	−53.86		
				C	−97.29		
Ag_9^+	BP86	TZP	TZP	S		−301.22	−407.03
				N		−359.06	−406.49
				C		−359.23	
				S	−369.08		
				N	−373.39		
				C	−417.20		
Ag_{23}	BP86	TZP	TZP	S		−61.43	−116.41
				N		−97.97	−122.21
				S	−118.43		
				N	−113.08		
Ag_{23}^+	BP86	TZP	TZP	S		−287.83	−363.38
				N		−328.13	−373.16
				S	−343.13		
				N	−343.58		

a small energy difference, which can be explained by the poor description of the Ag atom itself (using a 3-21G basis set). One should note that an interaction via the carbon atom is found to be unstable. The geometry optimization leads to an interaction via the sulfur atom or via the nitrogen atom.

Comparing these results with these of Pacchioni et al.,[27] one can see that the geometry for a S interaction was well-predicted; however, the nonlinear geometry for a N interaction was not recovered. As is seen in our own HF results, this can be attributed to effects of electron correlation.

Study of the Ag_9 Cluster. The Ag_9 cluster was built in such a way that a two-layer cluster with two adsorption sites was obtained (see Figure 6), on one side an atop and on the other a hollow site. Also, the bridge site can be found on this cluster, although this site includes an edge atom. Constraints similar to the previous cases were again used. When one looks to the atop site, a preferred adsorption via N over adsorption via S is noticed.

The preferred interaction on the hollow site occurs when the carbon atom is found above this specific site (see Table 3). This interaction energy is again expected to be enhanced by overbinding at the edge atoms. Because SCN^- possesses a quite strong dipole moment (6.6223 au B3PW91/6-311+G* with respect to the center of mass), it is expected to orient along the applied electrostatic field of the electrode and not perpendicular[19] to it, stabilizing the adsorption geometry perpendicular to the surface over the geometry parallel to the surface.

When one compares the N versus S interaction at the hollow site, a preferred interaction via S is found. On a cluster with a single positive charge, one observes a slight preference for adsorption via N. The fact that the hollow site prefers S adsorption can be explained by the fact that sulfur can be more easily five-coordinated than nitrogen but also in terms of hard and soft acids and bases (HSAB principle) proposed by Pearson[52,53] as will be seen in the case of the final cluster.

When the interaction energy at both sites (atop and hollow) on the same cluster is compared, adsorption at the hollow site is found to be the most stable. In the calculation discussed in the next section, an even larger Ag cluster was used to avoid cluster size effects.

Study of the Ag_{23} Cluster. A Ag_{23} cluster was constructed (see Figure 7) so that the central atoms at which adsorption occurs are coordinated to a maximal extent. In this calculation, edge effects are eliminated as much as possible. The Ag_{23} cluster was the largest possible model from a quality/cost ratio point of view.

On the uncharged cluster, an interaction via the nitrogen atom on the atop site and one via the sulfur atom on the hollow site are preferred (see Table 3). When the interaction energies at the hollow and atop site are compared, it can be seen that an interaction via the sulfur atom at the hollow site is preferred, in agreement with the results for the Ag_9 cluster. On a positively charged cluster, the hollow site is still preferred, but interaction via N becomes stronger than that via S, as is the case for the Ag_9 cluster, but the difference is only 0.4 kJ/mol. Increasing the surface charge seems to stabilize adsorption via N more than that via S. This observation is in line with Pearson's HSAB principle.[52,53] In our previous studies on the Fukui functions,[54,55] it was shown that in SCN^- the sulfur atom was softer than the nitrogen atom, the most reliable values being 0.677 au for the condensed Fukui function, f_S^- as compared to a 0.342 au for f_N^- (QCISD/aug-cc-pVDZ level values using Bader's population analysis[56]). When the charge of the surface is increased or the surface enlarged, the surface becomes "harder" and an interaction via the harder nitrogen atom is preferred to on via the softer sulfur. Increasing the size of the adsorption cluster introduces the possibility to transfer more charge to the specific adsorption site, making it more positive (i.e., harder) and N to S adsorption. It is generally expected that the surface charge of an electrode is very low, much closer to zero than to +1. On the basis of interaction energies, adsorption via S at the hollow site is thus predicted to be favored. It will be shown that this is in full agreement with the obtained vibrational spectra. Increasing the potential, making the surface more positive, would stabilize the interaction via N more than the interaction via S. At extremely high potential, the preferred adsorption geometry is thus expected to change from via S to via N. It, however, is not possible to verify this finding experimentally because of the oxidation of the Ag electrode at high potentials.

All of this shows that the charge of the silver electrode is so low that it can be modeled best by neutral clusters. The adsorption site is very important because the hollow and the atop site have a different affinity to SCN^-. If a silver surface was constructed of only atop sites, adsorption via N would be preferred. Also, the cluster size, as well as the calculation level, is important in this kind of calculations in which the energy

TABLE 4: Calculated Geometry (Distances, *D*, in Å), Energy (*E*, au) and Vibrational Frequencies (ν, cm^{-1}) of SCN^- and the Differences between Theoretical and Experimental CS and CN Frequencies ($\Delta\nu$) and the MRD (see text)

	D(S−C)	*D*(C−N)	*E*	ν	$\nu - \nu_{exptl}$	MRD (%)
exptl ν(CS)				756		
exptl ν(CN)				2059		
HF/3-21G*	1.682	1.153	−487.504 735	734	−22	10.1
				2414	355	
B3PW91/3-21G*	1.664	1.186	−488.638 187	751	−5	2.7
				2155	96	
B3PW91/6-31G*	1.668	1.181	−491.009 778	750	−6	3.5
				2185	126	
B3PW91/6-31+G*	1.664	1.183	−491.025 296	748	−8	2.8
				2153	94	
B3PW91/6-311+G*	1.660	1.176	−491.071 963	750	−6	2.5
				2146	87	
B3PW91/LanL2DZ	1.715	1.202	−102.976 749	689	−67	5.0
				2080	21	

differences between the different geometries are only a few kJ/mol, although the trends are predicted accurately on a small Ag_9 cluster, if interaction with edge atoms is avoided.

3. Frequencies. *Theoretical Results and Frequency Shift Analysis.* The frequency calculations were performed at two different levels, using the B3PW91/6-311+G*/3-21G and the B3PW91/LanL2DZ methods. The frequencies for the CS and CN stretch were considered, as well as their frequency shift after interaction with Ag.

Surface clusters containing up to five silver atoms were considered, and a final check was made with a Ag_9 cluster calculation. Small clusters can provide useful information Because frequency calculations are less dependent on the cluster size.[57,58]

The results for the free SCN^- have a mean relative deviation (MRD) with experiment of 2.5% and 5.0% for B3PW91/6-311+G*/3-21G (6-311+G*/3-21G for SCN^- and Ag, respectively) and the B3PW91/LanL2DZ method, respectively. The best performing basis set is the Pople one, as could be expected (see Table 4).

When one looks at the results for the adsorption complexes (see Table 5), the frequency shifts for the interaction on a neutral as well as for that on the positively charged clusters are in very good agreement with experiment if interaction occurs via S. Experimentally, the CS frequency shifts to lower wavenumbers and the CN shifts to to higher wavenumbers relative to the free SCN^-. For the complexes in which the interaction is via sulfur, the experimental trend is reproduced. For the interaction via the nitrogen, the opposite shifts are observed on all clusters.

From the frequency calculations, it can be concluded that SCN is orthogonal to the surface and binds via its sulfur site. The results of the frequency calculations are in full agreement with the interaction energy calculations on the neutral clusters in which the interaction via S at the hollow site is always found to be preferred (see Table 5).

The evolution of the wavenumber as a function of the electrode charge (Figure 8) shows that the C≡N stretching wavenumber increases further with a less negative potential on the electrode. If we compare the calculated C−N frequency shifts with the neutral and the charged cluster, this trend is reproduced by the calculation. For the Ag_2 cluster with interaction via S, the frequency shift goes from +58 to +95 and +131 cm^{-1} when the charge is increased from 0 to +1 and +2. The same is found for the Ag_4 cluster (+23 to +66 cm^{-1}) and for the Ag_5 cluster (+4 to +22 cm^{-1}). The experimental trend for the SC vibration is less clear but points into the direction of a decrease in wavenumber with increasing potential, which is also found in the calculations. The increase in C≡N frequency upon adsorption indicates a strengthening of the CN bond in SCN^- after interaction. The change in calculated bond length upon adsorption (d_{CN} = 12.02 pm becomes 11.94 pm, this difference is significant because CN is a triple bond) also indicates this strengthening. This behavior can be explained in terms of the following two canonical forms for SCN^-:

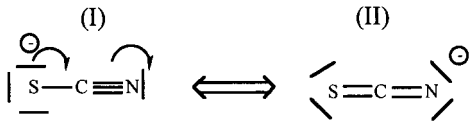

The higher softness of sulfur compared to nitrogen[54] means that S can manage a negative charge more easily, causing the

TABLE 5: Vibrational Frequencies (ν, cm^{-1}) and Frequency Shifts ($\Delta\nu$) of the SC and CN Vibrations of SCN^- in Interaction with the Different Clusters and for Different calculation methods[a]

	*n*Ag charge	ν(C−S)	ν(C−N)	$\Delta\nu$(C−S)	$\Delta\nu$(C−N)
exptl values SCN		756	2059		
exptl values interaction		723	2104	−33	45
		SCN			
B3PW91/6-311+G*	0	750	2146		
B3PW91/LanL2DZ	0	689	2080		
		NCS···Ag			
B3PW91/6-311+G*	+1	713	2223	−37	77
B3PW91/LanL2DZ	+1	654	2174	−35	94
B3PW91/6-311+G*	0	737	2180	−12	35
B3PW91/LanL2DZ	0	673	2119	−16	39
		SCN···Ag			
B3PW91/6-311+G*	+1	897	2139	147	−7
B3PW91/LanL2DZ	+1	828	2059	139	−20
B3PW91/6-311+G*	0	808	2154	58	8
B3PW91/LanL2DZ	0	736	2103	47	23
		NCS···Ag_2			
B3PW91/6-311+G*	+2	692	2267	−58	121
B3PW91/LanL2DZ	+2	636	2211	−53	131
B3PW91/6-311+G*	+1	714	2226	−36	81
B3PW91/LanL2DZ	+1	651	2175	−38	95
B3PW91/6-311+G*	0	735	2192	−15	47
B3PW91/LanL2DZ	0	668	2137	−21	58
		SCN···Ag_2			
B3PW91/6-311+G*	+2	959	2033	209	−113
B3PW91/LanL2DZ	+2	892	1987	204	−93
B3PW91/6-311+G*	+1	885	2064	135	−82
B3PW91/LanL2DZ	+1	798	2051	109	−29
B3PW91/6-311+G*	0	825	2162	136	82
B3PW91/LanL2DZ	0	764	2120	76	40
		NCS···Ag_4			
B3PW91/LanL2DZ					
S	+1	589	2146	−100	66
N	+1	784	1914	95	−166
S	0	622	2103	−67	23
N	0	733	2010	44	−70
C	0	687	2075	−1	−4
		NCS···Ag_5			
B3PW91/LanL2DZ					
S (atop)	+1	663	2102	−26	22
N (atop)	+1	770	2021	81	−59
S (bridge)	0	724	1925	35	−155
S (atop)	0	668	2084	−21	4
N (bridge)	0	657	2100	−32	20
N (atop)	0	736	2015	47	−65
C	0	669	2068	−19	−12
		NCS···Ag_9			
S (atop)	0	668	2105	−21	25

[a] Geometries are illustrated in Figures 2−7.

first canonical form (I) to be dominant. After interaction, the following canonical forms can be written:

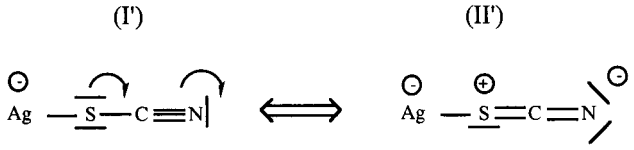

The second canonical form (II′) of $AgSCN^-$ is now even less favorable (due to the partial charges on the different atoms) so that the triple bond character of the CN bond is increased compared to the uncomplexed case. At the same time, the CS bond has less double bond character, both tendencies being in agreement with the experimental and theoretically observed frequency shifts in case of adsorption via the sulfur atom.

Conclusion

Combination of SER experimental and theoretical results allowed us to unambiguously determine the preferred adsorption site and geometry of SCN^- on a silver electrode. SCN^- adsorbs via its sulfur atom at the hollow site of the Ag(100) surface. The frequency shifts upon changing the potential of the silver electrode were also reproduced by our theoretical calculations.

An ab initio, DFT-based study on the SCN^- adsorption on a transition metal electrode is presented, using clusters containing up to 23 Ag atoms. The interaction energy of the SCN^- with different Ag clusters was calculated at different DFT levels. It is possible to obtain good relative adsorption energies already with a limited sized cluster (Ag_9); however, one should be aware of overbinding by edge atoms. For good quantitative adsorption energies, large, well-constructed clusters (e.g., Ag_{23}) are necessary. In a second part, the shift of the vibrational frequencies upon adsorption was calculated for different adsorption sites, geometries, and surface charges.

Finally, it was shown that the charge of the silver atoms is important for the final adsorption geometry. If the surface charge becomes significantly positive, adsorption via nitrogen becomes favorable over adsorption via sulfur. The latter could be explained in terms of the HSAB principle. Such high charges cannot be observed experimentally, however.

Acknowledgment. F.T. thanks the Flemish Institute for support of Scientific-Technological Research in Industry (I.W.T.) for a postdoctoral fellowship. M.S. thanks the FWO Flanders for a predoctoral fellowship. E.T. thanks the Flemish Institute for support of Scientific-Technological Research in Industry (I.W.T.) for a predoctoral fellowship. P.G. is indebted to the Free University of Brussels for a generous computer grant and to the F.W.O. Flanders for continuous support. The authors thank a referee for his constructive remarks.

References and Notes

(1) James, T. H. In *The Theory of the Photographic Process*, 4th ed.; James, T. H., Ed.; Macmillan: New York, 1977.
(2) Matejec, R. In *Photographic Silver Halide Diffusion Processes*; Rott, A., Weyde, E., Eds.; Focal Press: London, 1972; Chapter 6.
(3) Kraft, W. In *Photographic Silver Halide Diffusion Processes*; Rott, A., Weyde, E., Eds.; Focal Press: London, 1972; Chapter 3.2.
(4) Levenson, G. I. P. In *The Theory of the Photographic Process*, 4th ed.; James, T. H., Ed.; Macmillan: New York, 1977.
(5) Weyde, E.; Klein, E.; Metz, H. J. *J. Photogr. Sci.* **1962**, *10*, 110.
(6) Gonissen, D.; Hubin, A.; Vereecken, J. *Electrochim. Acta* **1996**, *41*, 1051.
(7) Vandeputte, S.; Tribollet, B.; Hubin, A.; Vereecken, J. *Electrochim. Acta* **1994**, *39*, 2729.
(8) Gonnissen, D.; Hubin, A.; Vereecken, J. *Electrochim. Acta* **1999**, *44*, 4129.
(9) Simons, W.; Gonnissen, D.; Hubin, A. In *ECS Proceedings of the Joint International Meeting of the Electrochemical Society and International Society of Electrochemistry*, Paris, 1997; Paunoric, M., Datta, M., Matlosc, M., Osaka, T., Talbot, J. B., Eds.; 1997; Vol. 27, p 124.
(10) Gonnissen, D.; Langenaeker, W.; Hubin, A.; Geerlings, P. *J. Raman Spectrosc.* **1998**, *29*, 1031.
(11) Markovits, A.; Garcia-Hernandez, M.; Ricart, J. M.; Illas, F. *J. Phys. Chem. B* **1999**, *103*, 509.
(12) Garcia-Hernandez, M.; Curulla, D.; Clotet, A.; Illas, F. *J. Chem. Phys.* **2000**, *113*, 364.
(13) Koper, M. T. M.; van Santen, R. A.; Wasileski, S. A.; Weaver, M. J. *J. Chem. Phys.* **2000**, *113*, 4392.
(14) Sauer, J.; Ugliengo, P.; Garonne, E.; Saunders, V. R. *Chem. Rev.* **1994**, *94*, 2095.
(15) Parr, R. G.; Yang, W. *Density-Functional Theory of Atoms and Molecules*; Oxford University Press: New York, 1989.
(16) Chermette, H. *J. Comput. Chem.* **1999**, *20*, 129.
(17) Neurok, M. *Stud. Surf. Sci. Catal.* **1997**, *109*, 3.
(18) Balbuena, P. B.; Derosa, P. A.; Seminario, J. A. *J. Phys. Chem. B* **1999**, *103*, 2830.
(19) Crispin, X.; Bureau, C.; Geskin, V. M.; Lazzaroni, R.; Salaneck, W. R.; Bredas J. L. *J. Chem. Phys.* **1999**, *111*, 3237.
(20) Mittendofer, F.; Hafner, J. *Surf. Sci.* **2001**, *472*, 133.
(21) Hammer, B.; Nørskov, J. K. *Adv. Catal.* **2000**, *45*, 71.
(22) Lee, S. B.; Kim, K.; Kim, M. S.; Oh, W. S.; Lee, Y. S. *J. Mol. Struct. (THEOCHEM)* **1995**, *296*, 5.
(23) Nakatsuji, H.; Nakai, H. *J. Chem. Phys.* **1998**, *98*, 2423.
(24) Ignaczak, A.; Gomes, J. A. N. F. *J. Electroanal. Chem.* **1997**, *420*, 71.
(25) Ignaczak, A.; Gomes, J. A. N. F. *J. Electroanal. Chem.* **1997**, *420*, 209.
(26) Ignaczak, A. *J. Electroanal. Chem.* **2000**, *480*, 209.
(27) Pacchioni, G.; Illas, F.; Philpott, M. R.; Bagus, P. S. *J. Phys. Chem.* **1991**, *95*, 4678.
(28) Geerlings, P.; De Proft, F.; Langenaeker, W. *Adv. Quantum Chem.* **1999**, *33*, 303.
(29) Geerlings, P.; De Proft, F. *Int. J. Quantum Chem.* **2000**, *80*, 227.
(30) De Proft, F.; Geerlings, P. *Chem. Rev.* **2001**, *101*, 1451.
(31) Balawender, R.; Safi, B.; Geerlings, P. *J. Phys. Chem. A* **2001**, *105*, 6703 and references therein.
(32) Perdew, J. P. *Phys. Chem. Rev. B* **1986**, *33*, 8822.
(33) Stephens, P. J.; Delvin, F. J.; Chablowski, C. F.; Frisch, M. J. *J. Phys. Chem.* **1994**, *98*, 11623.
(34) Ricca, A.; Bauschlicher, C. W. *J. Phys. Chem.* **1994**, *98*, 12899.
(35) Russo, T. V.; Martin, R. L.; Hay, P. J. *J. Chem. Phys.* **1995**, *102*, 8023.
(36) Siegbahn, P. E. M.; Crabtree, R. H. *J. Am. Chem. Soc.* **1997**, *119*, 3103.
(37) Yanagisawa, S.; Tsuneda, T.; Hirao, K. *J. Chem. Phys.* **2000**, *112*, 545.
(38) Barden, C. J.; Rienstra-Kiracofe, J. C.; Schaefer, H. F., III *J. Chem. Phys.* **2001**, *113*, 690.
(39) te Velde, G.; Bickelhaupt, F. M.; Baerends, E. J.; Fonseca Guerra, C.; Van Gisbergen, F. J. A.; Snijders, J. G.; Ziegler, T. *J. Comput. Chem.* **2000**, *22*, 931.
(40) van Lenthe, E.; van Leeuwen, R.; Baerends, E. J.; Snijders, J. G. *Int. J. Quantum Chem.* **1996**, *57*, 281.
(41) Hehre, W. J.; Radom, L.; Schleyer, P. v. R.; Pople, J. A. *Ab Initio Molecular Orbital Theory*; John Wiley: New York, 1986.
(42) Hay, P. J.; Wadt, W. R. *J. Chem. Phys.* **1985**, *82*, 270.
(43) Wadt, W. R.; Hay, P. J. *J. Chem. Phys.* **1985**, *82*, 284.
(44) Hay, P. J.; Wadt, W. R. *J. Chem. Phys.* **1985**, *82*, 299.
(45) Frisch, M. J.; Trucks, G. W.; Schlegel, H. B.; Scuseria, G. E.; Robb, M. A.; Cheeseman, J. R.; Zakrzewski, V. G.; Montgomery, J. A., Jr.; Stratmann, R. E.; Burant, J. C.; Dapprich, S.; Millam, J. M.; Daniels, A. D.; Kudin, K. N.; Strain, M. C.; Farkas, O.; Tomasi, J.; Barone, V.; Cossi, M.; Cammi, R.; Mennucci, B.; Pomelli, C.; Adamo, C.; Clifford, S.; Ochterski, J.; Petersson, G. A.; Ayala, P. Y.; Cui, Q.; Morokuma, K.; Malick, D. K.; Rabuck, A. D.; Raghavachari, K.; Foresman, J. B.; Cioslowski, J.; Ortiz, J. V.; Stefanov, B. B.; Liu, G.; Liashenko, A.; Piskorz, P.; Komaromi, I.; Gomperts, R.; Martin, R. L.; Fox, D. J.; Keith, T.; Al-Laham, M. A.; Peng, C. Y.; Nanayakkara, A.; Gonzalez, C.; Challacombe, M.; Gill, P. M. W.; Johnson, B. G.; Chen, W.; Wong, M. W.; Andres, J. L.; Head-Gordon, M.; Replogle, E. S.; Pople, J. A. *Gaussian 98*, revision A.6; Gaussian, Inc.: Pittsburgh, PA, 1998.
(46) Boys, S. F.; Bernardi, F. *Mol. Phys.* **1970**, *19*, 553.
(47) For an overview, see: Van Duijnveldt, F. B.; Van Duijnveldt-Van De Rijdt, J. G. C. M.; Van Lenthe, J. H. *Chem. Rev.* **1994**, *94*, 1973.
(48) Trasatti, S. *Electrochim. Acta* **1992**, *37*, 2137.

(49) Wittbrodt, J. M.; Schlegel, H. B. *J. Chem. Phys.* **1996**, *105*, 6574.
(50) Smithells, M. J. *Metal Reference book*, 6th ed.; Butterworths: Washington, DC, 1983.
(51) Pearson, R. G. *J. Phys. Chem.* **1994**, *98*, 1989.
(52) Pearson, R. G. *Inorg. Chim. Acta* **1995**, *240*, 93.
(53) De Proft, F.; Martin, J. M. L.; Geerlings, P. *Chem. Phys. Lett.* **1996**, *256*, 400.
(54) Geerlings, P.; De Proft, F.; Martin, J. M. L. In *Recent Developments and Applications of Modern Density Functional Theory*; Seminario, J. M., Ed.; Theoretical and Computational Chemistry, Vol. 4; Elsevier: Amsterdam, 1996; p 773.
(55) Lee, H. M.; Kim, M. S.; Kim, K. *Vib. Spectrosc.* **1994**, *7*, 175.
(56) Bader, R. F. W. *Atoms in Molecules, A Quantum Theory*; Clarendon Press: Oxford, U.K., 1990; p 182.
(57) Papai, I.; Ushio, J.; Salahub, D. R. *Surf. Sci.* **1993**, *282*, 262.
(58) Van Santen, R. A.; Neurock, M. *Catal. Rev.* **1995**, *37*, 557.